Droop Control Algorithm Design for Power Balancing in Island Inverter Based Microgrid

Jaroslav DRAGOUN, Martin VINS, Jakub TALLA, Vojtech BLAHNIK
University of West Bohemia, Faculty of Electrical Engineering, Pilsen 301 00, Czech Republic
dragounj@fel.zcu.cz

***Abstract*—In this article, a droop control algorithm is proposed for power distribution between sources in an island inverter-based microgrid without common central control. The analyses of the line impedance influence (resistive, inductive, and combined) are provided to show the impact on the power flow between a grid and a converter. Line impedance character influences the droop control algorithm performance. The impact of the accuracy of the setting, concerning line impedance, of the proposed droop control algorithm is then tested in a simulation. For the simulation, a microgrid model was built in the Simulink environment (MATLAB) with the PLECS toolbox. In the conclusion, the potential benefits and applications of the proposed droop control are discussed.**

***Index Terms*—control algorithm, droop control, line impedance, microgrid, power balancing.**

I. INTRODUCTION

The majority share of fossil fuels in energy generation in the past led to environmental pollution and with high certainty also to the induction of climate change. However, in the future, the energy generation by these classical non-renewable energy sources (gas, coal, and diesel) is unsustainable due to previously mentioned factors as well as due to their exhaustion [1-4].

In reaction to that, renewable energy sources (RES) have been gaining more attention. The popularity of the RES also led to the rise of distributed generation (DG) systems development enabling easier integration of RES into the electrical grid [5-8].

Highly reliable electric power can be provided by DG systems [9]. Sources such as photovoltaic panels, small wind turbines, fuel cells, etc. can be considered as well as energy storage systems [10]. Because it is difficult to connect these RES directly to the electrical grid [11-12] the interface between them and the electrical grid is called a microgrid as can be seen in Fig. 1.

Microgrid generally consists of several DG systems (sources or energy storage systems) and loads. More distributed sources provide greater supply reliability in the case of a failure of any of them. Regarding Fig. 1 microgrid can be connected or disconnected from the grid [13-14]. Followingly the main advantage of the standalone (disconnected) DG systems lies in significantly better control options and power flexibility [15] in the following text this system is called islanded microgrid.

It is evident the majority of DG (or storage systems), such as photovoltaics and batteries, provide direct current (DC) power.

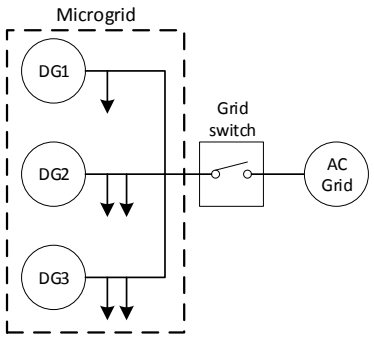

Figure 1. Microgrid with possible grid connection illustration

This makes inverter a crucial component of microgrids [16-17]. Due to the basic microgrid topology, inverters are connected in parallel. This connection means that even a small difference in the converter output voltage can lead to a great difference in output power.

A couple of control techniques have been described for microgrids consisting of multiple parallel inverters [18-20], or [21]. Although these control techniques work well for the microgrid with central control, droop control (voltage and frequency) is one of the most popular [22] and can work without central control as well. It can be said that centralized control provides more accurate power control and power flow optimization compared to decentralized control. The benefit of decentralized control is its simplicity, which allows for example fast integration of new sources to the microgrid. Another of the benefits of droop control is its familiarity with the professional public, because it is commonly used in the control of synchronous generators in power plants.

Droop control can be also applied in the control of grid-connected inverter-based power sources. Following the same principles as in the case of the synchronous generators, the active power is controlled by changing the output frequency. This leads to the increasing phase shift between the voltage of the source and the grid [22-24].

A lot of work is done dealing with droop control technique modifications [22]. There are such types as conventional droop control [22], [25], virtual impedance droop control [22], [26], or adaptive and robust droop control [22], [27]. However, a lot of works dealing with virtual impedances are not considering microgrids without a strong voltage source (usually public power grid) [22], [28-29]. So, these algorithms cannot be used in islanded microgrids, but the importance of these island microgrids will grow with increasing RES integration and efforts to

This research has been supported by the Ministry of Education, Youth and Sports of the Czech Republic under the project OP VVV Electrical Engineering Technologies with High-Level of Embedded Intelligence CZ.02.1.01/0.0/0.0/18_069/0009855 and by the UWB Student grant project no. SGS-2021-021.

Digital Object Identifier 10.4316/AECE.2022.04008

supply quality electric power [30-31].

Most of the work regarding droop control neglects the influence of the line impedance character on the power flow. It considers purely inductive character. In this paper droop control accounting for line impedance character is used and it is adapted for the power distribution between multiple converters without common superior control or communication. The proposed algorithm allows the creation of the islanded microgrid where the sources can be added without big changes in the current infrastructure. The microgrid will naturally include new sources in the power-balancing process. This paper also includes an analysis of the incorrect setting of the line impedance character in the droop control algorithm.

Section II discusses the basic operation of droop control. The influence of the line impedance on the power flow is analyzed in section III. Commonly used versions of droop control for the control of grid-connected converters are analyzed in section IV. A droop control designed for power balancing in islanded inverter-based microgrids is proposed in section V. Simulations verifying balancing capability and showing the influence of different settings of the droop control algorithm are provided in section VI.

II. Droop Control Introduction

The droop control method is used for the control of the power flow from the voltage source to the grid. It uses alteration of voltage drop on the line impedance. To explain this, a simple example will be used. Let's take a simple one-phase system shown in Fig. 2. The voltage source on the left represents a source of controlled voltage (voltage source inverter, generator). The voltage source on the right represents a grid voltage. The impedance in between represents a line impedance.

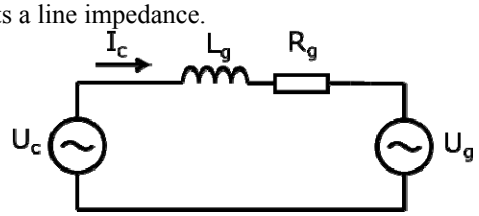

Figure 2. Droop control example

The total power exchanged with the grid can be calculated according to (1), because the U_g is given by the grid, the only way to control the power flow is to control the converter output current which is linked to the voltage drop on the line impedance (2).

There are two ways, how to change the converter voltage to achieve power flow control. The magnitude difference and the phase shift between the grid and converter voltage controls the active and the reactive power flow. It depends on the line impedance character if the magnitude difference controls the active power, the reactive power, etc.

$$\overline{S} = \overline{U_g} \cdot \overline{I_c} \tag{1}$$

$$\overline{I_c} = \frac{\overline{U_c} - \overline{U_g}}{\overline{Z_g}} \tag{2}$$

III. Influence of Line Impedance

To show the influence of different line impedances on the active and reactive power flow, simple examples in the complex plane are shown. In these illustrative examples a purely resistive, or a purely inductive line impedance is assumed as shown in Fig. 3. The converter output current I_c is caused by a difference between converter voltage phasor U_c and grid voltage phasor U_g. In the case of the inductive line impedance, reactive power is exchanged with the grid (phase shift between grid voltage and current is 90°). In the case of resistive line impedance, active power is exchanged with the grid.

Fig. 4 shows the converter output current caused by a phase shift between the converter and grid voltage. This leads to the opposite result, compared to the magnitude difference. In the case of inductive line impedance phase shift leads to an exchange of active power. In the case of resistive line impedance phase shift leads to an exchange of reactive power. In Fig. 4 it can also be seen that in this case, the power flow is not purely active or reactive. This effect can be neglected for a small phase shift angle, but with a growing angle, grows its significance.

Fig. 5 shows that for a combination of resistive and inductive line impedance, resulting in that the power flow is also a combination of active and reactive power, both for magnitude and phase shift difference.

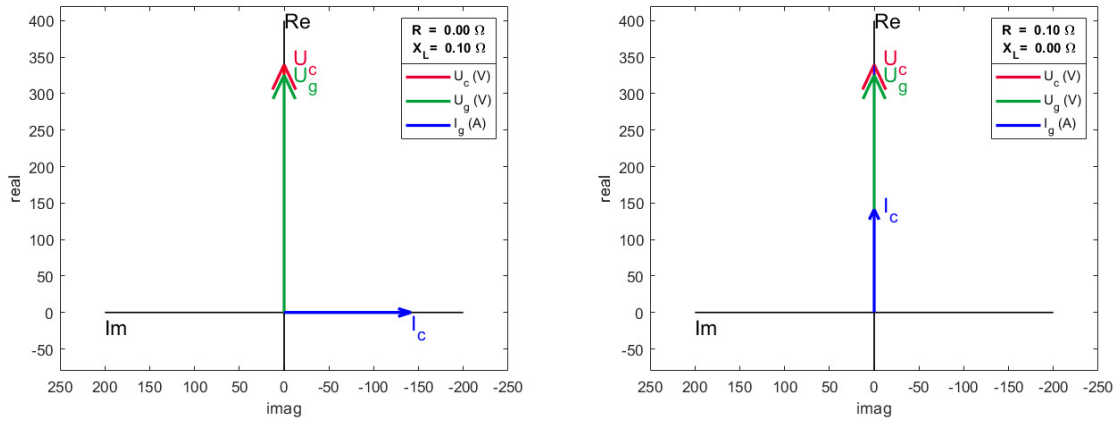

Figure 3. Magnitude difference influence on power flow for different line impedance

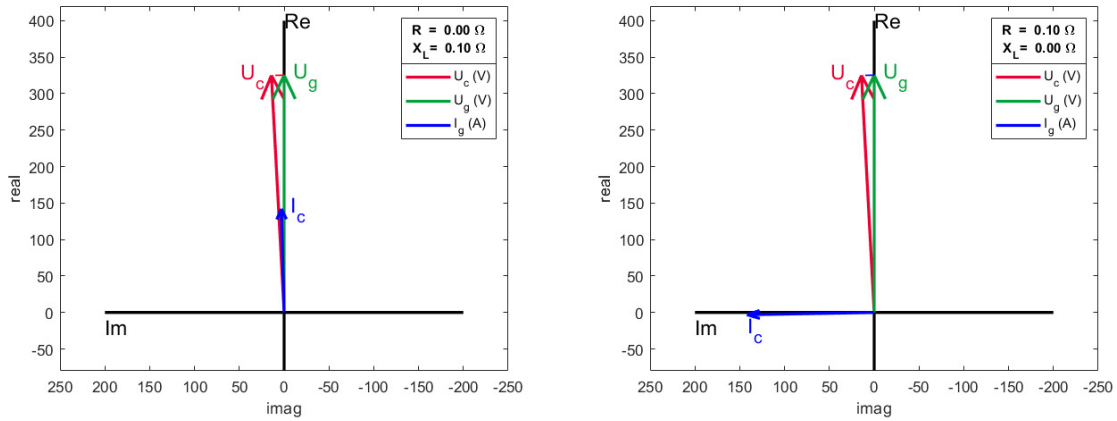

Figure 4. Phase shift difference influence on power flow, for different line impedance

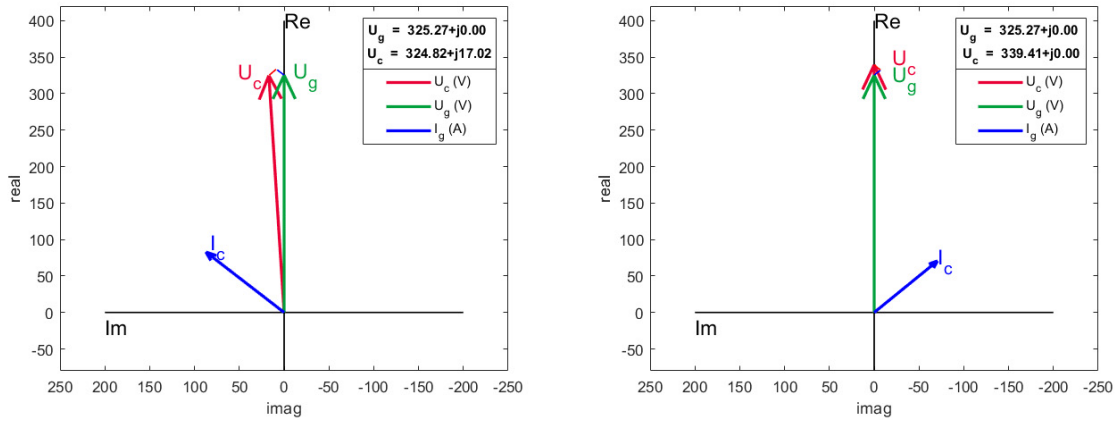

Figure 5. Phase shift and magnitude for RL impedance

IV. Droop Control Algorithms

Equation (3) describes the relations between the grid voltage u_g (V) and the converter voltage u_c (V). Voltage u_g calculation is based on grid voltage U_{mg} (V) magnitude and its phase shift ϑ_g (rad).

Voltage u_c is calculated based on the magnitude U_{mc} (V) and phase shift ϑ_c (rad), which are given by droop control shown in the following equations.

$$u_g = U_{m_g} \sin\left(\vartheta_g\right) \tag{3.1}$$

$$u_c = U_{m_c} \sin\left(\vartheta_c\right) \tag{3.2}$$

The behavior described in the previous section can be used to develop a power control algorithm. This algorithm consists of two PI controllers. Their input is actual and required output power divided into the active and reactive components. Commonly the resistive component of line impedance is ignored [32]. This approach is mainly applied for the control of generators, which have a dominant leakage inductance of stator winding, and for converters connected to the grid using a simple inductor as a filter. Equation (4) can be used in these cases. The calculation is based on grid voltage u_g (V), which consists of its magnitude U_{mg} (V) and angle of rotation ϑ_g (rad). Converter output voltage u_c (V) is controlled by the PI controller defined by the gain constants k, where k_{pP} and k_{pQ} are proportional gains for active and reactive power controllers. Constants k_{iP} and k_{iQ} are integral gains for active and reactive power controllers. The proportional and integral gains of the active and reactive power controllers are not the same. Gains depend on the parameters of the line impedance, the nominal output power of the controlled source, and the allowed range where can be parameters of the output voltage changed. Control error is calculated as the difference between actual output power P (W) or Q (var) and required output power P^* (W) or Q^* (var). Outputs of the controllers are the magnitude of the converter voltage U_{mc} (V) and its angle of rotation ϑ_c (rad).

$$\vartheta_c = \vartheta_g - \frac{k_{pP}s + k_{iP}}{s}(P - P^*) \tag{4.1}$$

$$U_{m_c} = U_{m_g} - \frac{k_{pQ}s + k_{iQ}}{s}(Q - Q^*) \tag{4.2}$$

This simplification leads to a slower reaction of the control loop. It neglects a coupling between a direct and quadrature component of the output voltage and current. This is a well-known problem linked to the use of voltage source converters [33]. Coupling can be considered by the inclusion of line impedance character resulting droop control is described by equations (5) [34-35]. In the equations, the angle θ represents the phase shift caused by the complex line impedance.

$$\vartheta_c = \vartheta_g - \frac{k_{pP}s + k_{iP}}{s}\left[(P - P^*)\sin(\theta) - (Q - Q^*)\cos(\theta)\right] \tag{5.1}$$

$$U_{m_c} = U_{m_g} - \frac{k_{pQ}s + k_{iQ}}{s} \cdot \cdot\left[(P - P^*)\cos(\theta) + (Q - Q^*)\sin(\theta)\right] \tag{5.2}$$

V. Proposed Droop Control

Equations (4) and (5) are suitable for applications, where precise power output control is needed, and the controlled

source is connected to the strong grid. An example of this can be the photovoltaic system, which needs a precise setting of output power for the maximum power point tracking algorithm [36]. These equations cannot be used in the case of the analyzed (developed) microgrid. It is based on multiple identical inverters. The only link between those converters is a three-phase AC grid. This means there is no strong source that could serve as a reference. Because there is no communication or superior control loop, the purpose of the droop control is in this case not to precisely control the output power, but to equalize the output power of individual converters.

The main difference of droop control used in this context is, that there is no reference for required output power. So, the required output power is set to zero, and the integrational part of the controller is disabled. The second difference is linked to the control of the phase shift. To get a phase shift between individual converter voltages, their output frequency must change.

With these changes considered, the final used droop control for the microgrid is described in (6).

$$\omega = \omega_n - k_{pP}\left[(P)\sin(\theta) - (Q)\cos(\theta)\right] \tag{6.1}$$

$$\vartheta = \frac{1}{s}\omega \tag{6.2}$$

$$E = E^* - k_{pQ}\left[(P)\cos(\theta) + (Q)\sin(\theta)\right] \tag{6.3}$$

VI. SIMULATIONS

In this section, the results of simulations regarding droop control are presented. Fig. 6 shows the used control diagram. In this diagram, it can be seen, that although proportional controllers for magnitude and frequency are used, the calculation of voltage vector angle transforms one of the controllers into the integrational controller.

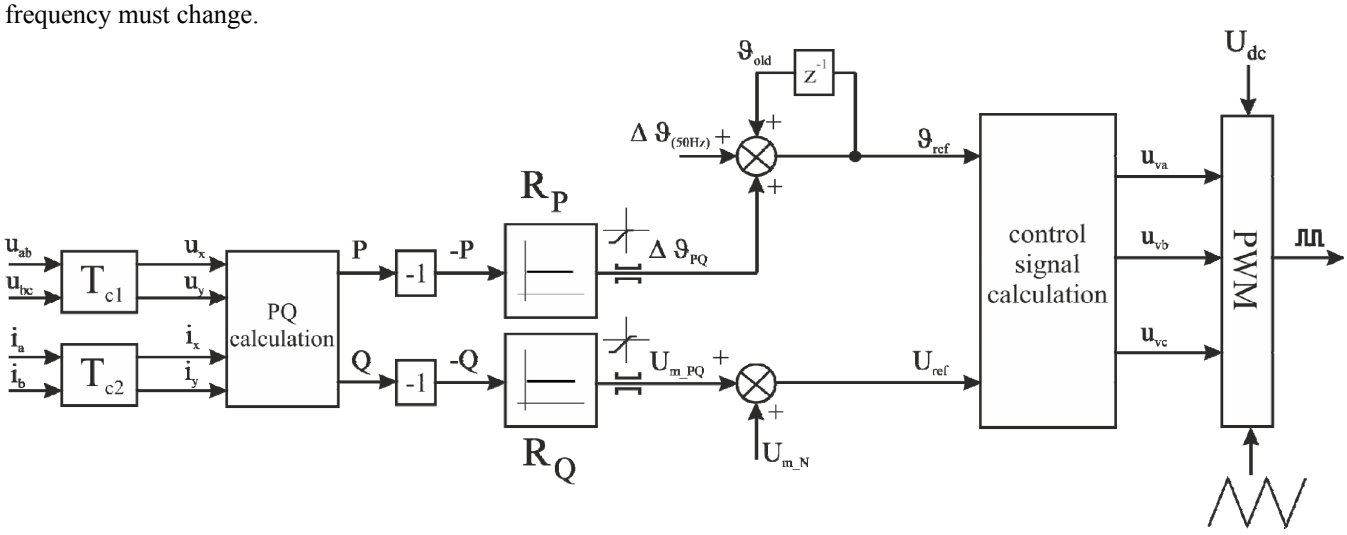

Figure 6. Control algorithm for microgrid droop control

Simulation is based on the example of the railway carriage microgrid used to power auxiliary drives. This united carriage microgrid provides a higher level of reliability in case of failure of one of the converters. Limiters used in droop control are set according to allowed deviations in the railway carriage microgrid. The output of the controller R_P has a limiter which ensures that the output voltage frequency does not drop under 49 Hz. Proportional gain is set to reach this limit at nominal active power output. By the summation of the $\Delta\vartheta_{(50Hz)}$ and $\Delta\vartheta_{PQ}$ (which determine the frequency of output voltage) with the value from the previous ϑ_{old}, the new value of the ϑ for the output voltage is calculated.

The output of controller R_Q has a limiter which ensures that the output voltage stays in the range from -25% U_n to +3% U_n. These margins are given by the application in a railway carriage microgrid.

In this part results of simulations will be discussed to verify the function of the proposed droop control. The Simulink (MATLAB) environment with the PLECS toolbox is used for model building and presented simulations. It contains six three-phase voltage sources controlled by the proposed droop control. These sources are connected to the common load via the lines with different impedances. The connection of six inverter cells with the common load is shown in Fig. 7.

Basic line parameters used in the simulation are shown in (7). Line parameters have a dominantly inductive character, which respects real applications in converter-based microgrids. In the simulated setup, the output impedance of the converters consists mostly of the output filter, but regarding the balancing algorithm, the main impact has the added line impedance Z_{line}, which is different for each converter. In comparison to reality, the resistive component of the Z_{line} is slightly boosted to show the benefit of the precise setting of the line impedance phase shift.

Impedance phase shift determines the coupling between output voltage parameters and output power flow. Impedance phase shift used in droop control does not have to match reality, this can be used to change the behavior of the droop control. The following simulations are examining the influence of different settings.

$$R_{line} = 17.5m\Omega \tag{7.1}$$

$$L_{line} = 180\mu H \rightarrow X_{L\_line} = 55.6m\Omega \tag{7.2}$$

$$\overline{Z_{line}} = R_{line} + j\omega L_{line} = 59.15e^{j1.27}m\Omega \tag{7.3}$$

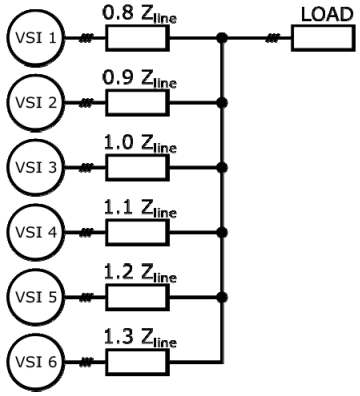

Figure 7. Representation scheme for droop control test

Equation (8) shows the formula used for the calculation of the difference in active power supplied by individual converters. Similarly, the reactive power and output current are calculated, as a difference from the mean value.

The first simulation result shows output powers and currents for the system with disabled droop control. In Fig. 8 and Fig. 9 the results of the simulation scenario are shown.

$$P_{mean} = \frac{\sum_{1}^{n} P_n}{n} \tag{8.1}$$

$$\Delta P_n = P_n - P_{mean} \tag{8.2}$$

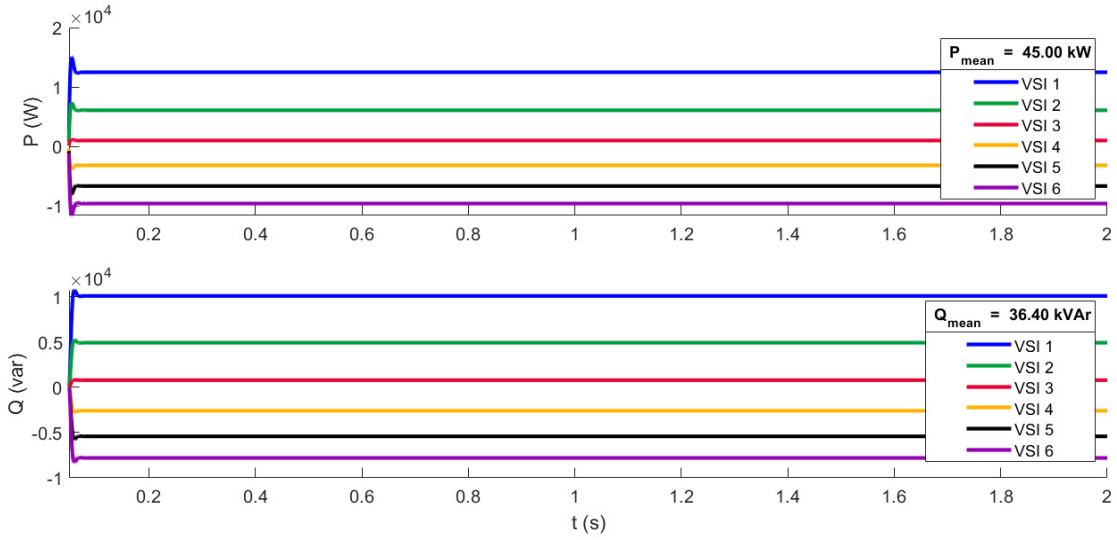

Figure 8. PQ difference with no droop control

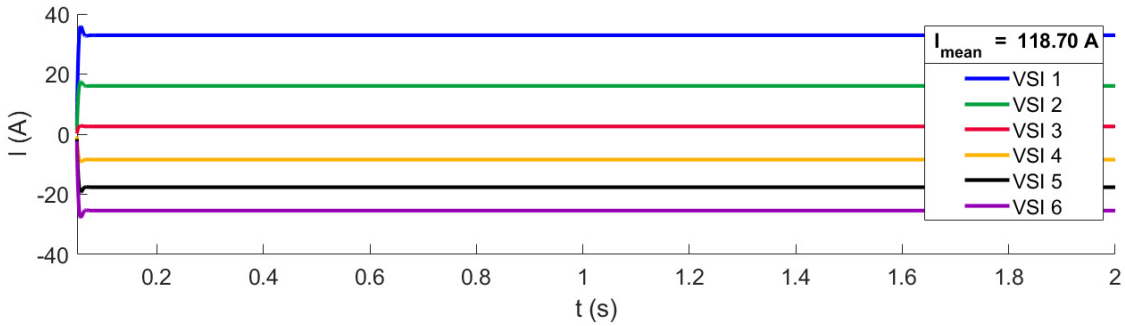

Figure 9. Output converter current difference with no droop control

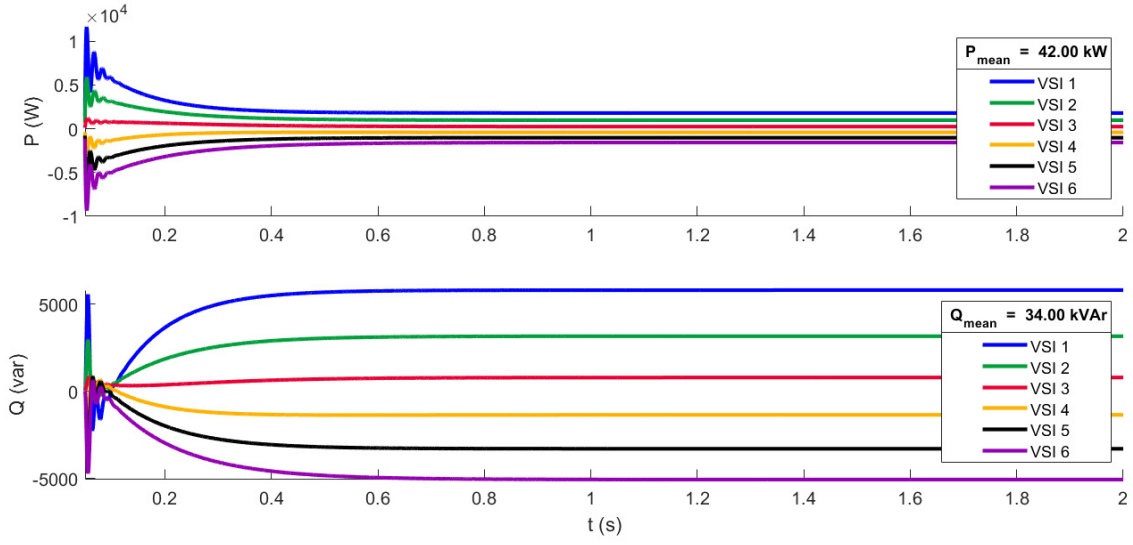

Figure 10. PQ difference with precise parametrization of droop control

Results with the precise setting of the droop control respecting actual parameters of line impedance are shown in Fig. 10 and Fig. 11. In this scenario, it is assumed, that the phase shift of the line impedance is known. This setting leads to the best performance regarding output current distribution among the microgrid converters. The precise setting of the droop control also leads to the fastest way to reach a steady-state.

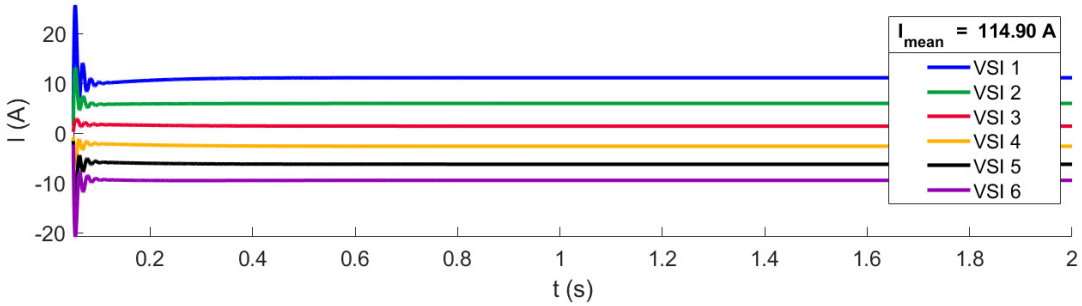

Figure 11. Output converter current difference with precise parametrization of droop control

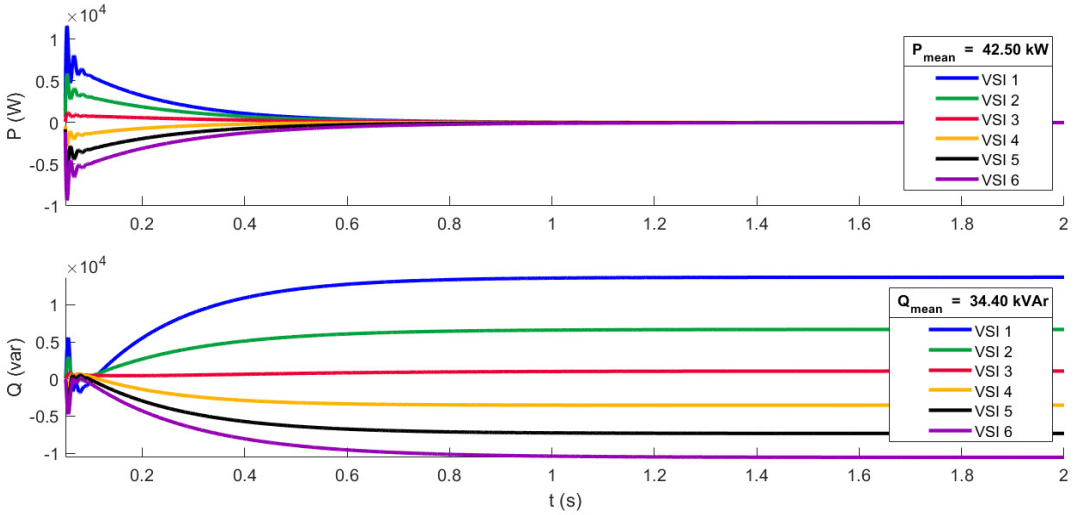

Figure 12. PQ difference with parametrization of droop control for purely inductive line impedance

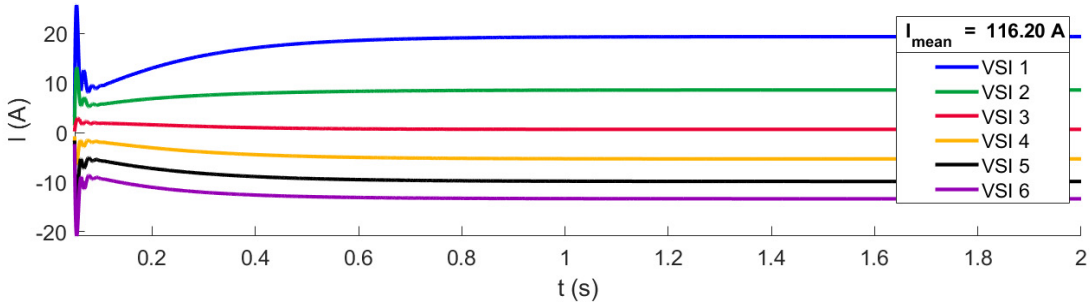

Figure 13. PQ difference with parametrization of droop control for purely inductive line impedance

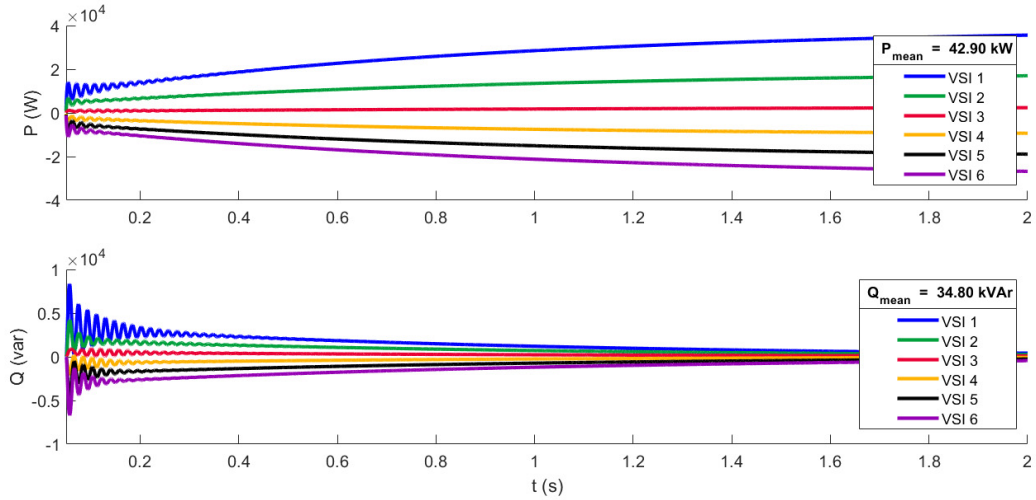

Figure 14. PQ difference with parametrization of droop control for purely resistive line impedance

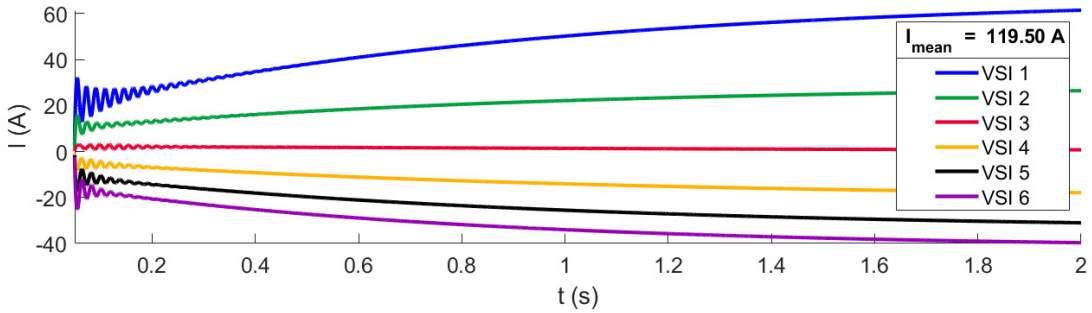

Figure 15. Output converter current difference with the setting of droop control for purely resistive line impedance

Because the line impedance is not always known, a test for incorrectly set line impedance angle has been performed. For the simulation, extreme cases have been tested, first is assuming purely inductive line character. The results are shown in Fig. 12 and Fig. 13. Integrative character of the phase shift control causes the difference of the active output power to reach zero in steady-state.

In contrast, another extreme case is assuming purely resistive line impedance. The results for this configuration are shown in Fig. 14 and Fig. 15.

VII. Conclusions

Section III describes an analysis of line impedance character influence on the power flow from the voltage source to the grid. This is a crucial factor in droop control algorithm behavior.

Despite that, line impedance character does not have to be followed exactly in process of droop control design. In this paper, there are examined the possibilities of the droop control alteration for the equalization of the output power of the individual sources in microgrids without superior control.

The presented simulation results show the operation of the proposed droop control without a reference signal from a superior control. The droop control in this context is used to equalize the power output of the controllers connected to the microgrid.

The simulation confirmed assumptions, that character of the control influences the distribution of the power among the converters. The controller, which controls voltage phase shift (output voltage frequency), has an integrative character. This can be seen in the results for the droop control parametrized for purely resistive and inductive loads where P or Q differences converge to zero. The magnitude controller has a proportional character which causes the offset of output power. This offset is necessary for the used droop control, which does not have a set required output power.

Results show that for the correct set droop control, there is the best output current balance result. If the droop control is parametrized for purely inductive line impedance, it provides the best results for active power balancing. This can be beneficial in some cases. For example, if there is assumed a microgrid based on battery energy storage systems.

The focus here would be on the uniform state of charge (SOC) of the individual storages. In the case, where the droop control is parametrized for purely resistive line impedance, there is the best reactive power balance. But there is a significant downfall, this setting is in most cases distant from real line impedance. The balance of output reactive powers leads to a great difference in output currents. The output currents difference is even greater than in the case with no droop control.

References

[1] H. Ritchie, M. Roser, “Fossil Fuels,” Saving Ourselves, 2017, pp. 31–55. doi:10.1142/9789813220768_0003

[2] F. Martins, C. Felgueiras, M. Smitkova, N. Caetano, ”Analysis of fossil fuel energy consumption and environmental impacts in european countries,” Energies 2019, 12,964. doi:10.3390/en12060964

[3] J. Kotcher, E. Maybah, W. T. Choi, “Fossil fuels are harming our brains: Identifying key messages about the health effects of air pollution from fossil fuels,” BMC Public Health, vol. 19, no. 1, 2019. doi:10.1186/s12889-019-7373-1

[4] F. P. Perera, “Multiple threats to child health from fossil fuel combustion: Impacts of air pollution and climate change,” Environmental Health Perspectives, vol. 125, no. 2, 2017, pp. 141–148. doi:10.1289/ehp299

[5] O. Kuik, F. Branger, P. Quirion, “Competitive advantage in the renewable energy industry: Evidence from a gravity model,” Renewable Energy, vol. 131, 2019, pp. 472–481. doi:10.1016/j.renene.2018.07.046

[6] N. L. Panwar, S. C. Kaushik, S. Kothari, “Role of renewable energy sources in environmental protection: A review,” Renewable and Sustainable Energy Reviews, vol. 15, no. 3, 2011, pp. 1513–1524. doi:10.1016/j.rser.2010.11.037

[7] Z. Abdmouleh, A. Gastli, L. Ben-Brahim, M. Haouari, N. Ahmed Al-Emadi, “Review of optimization techniques applied for the integration of distributed generation from renewable energy sources,” Renewable Energy, vol. 113, 2017, pp. 266–280. doi:10.1016/j.renene.2017.05.087

[8] C. D. Iweh, S. Gyamfi, E. Tanyi, E. Effah-Donyina, “Distributed generation and renewable energy integration into the grid: Prerequisites, push factors, practical options, issues, and merits,” Energies, vol. 14, no. 17, 2021, p. 5375. doi:10.3390/en14175375

[9] R. Lasseter, A. Akhil, C. Marnay, J. Stephens, “Integration of distributed energy resources. The CERTS microgrid concept,” 2002. doi:10.2172/799644

[10] D. Georgakis, S. Papathanassiou, N. Hatziargyriou, A. Engler and C. Hardt, "Operation of a prototype microgrid system based on micro-sources quipped with fast-acting power electronics interfaces," 2004 IEEE 35th Annual Power Electronics Specialists Conference (IEEE Cat. No.04CH37551), 2004, pp. 2521-2526 Vol. 4. doi:10.1109/PESC.2004.1355225

[11] M. Mehrasa, E. Pouresmaeil, B. Pournazarian, A. Sepehr, M. Marzband, J. P. S. Catalão, “Synchronous resonant control technique to address power grid instability problems due to high renewables penetration,” Energies, vol. 11, no. 9, 2018, p. 2469. doi:10.3390/en11092469

[12] D. J. Swider, et al., “Conditions and costs for renewables electricity grid connection: Examples in Europe,” Renewable Energy, vol. 33, no. 8, 2008, pp. 1832–1842. doi:10.1016/j.renene.2007.11.005

[13] A. Werth, N. Kitamura, I. Matsumoto, K. Tanaka, “Evaluation of centralized and distributed microgrid topologies and comparison to open energy systems (OES),” 2015 IEEE 15th International Conference on Environment and Electrical Engineering (EEEIC), 2015. doi:10.1109/eeeic.2015.7165211

[14] M. Y. Nguyen, T. Y. Yong, “A comparison of microgrid topologies considering both market operations and reliability,” Electric Power Components and Systems, vol. 42, no. 6, 2014, pp. 585–594. doi:10.1080/15325008.2014.880963

[15] Y. W. Li, C.-N. Kao, "An accurate power control strategy for power-electronics-interfaced distributed generation units operating in a low-voltage multibus microgrid," IEEE Transactions on Power Electronics, vol. 24, no. 12, 2009, pp. 2977–2988. doi:10.1109/tpel.2009.2022828

[16] X. Li, A. Dyśko, G. M. Burt, "Traveling wave-based protection scheme for inverter-dominated microgrid using mathematical morphology," IEEE Transactions on Smart Grid, vol. 5, no. 5, 2014, pp. 2211–2218. doi: 10.1109/tsg.2014.2320365

[17] K. Dang, X. He, D. Bi, C. Feng, "An adaptive protection method for the inverter dominated microgrid," 2011 International Conference on Electrical Machines and Systems, 2011. doi:10.1109/icems.2011.6073457

[18] K. T. Tan, X. Y. Peng, P. L. So, Y. C. Chu, M. Z. Q. Chen, "Centralized control for parallel operation of distributed generation inverters in microgrids," IEEE Transactions on Smart Grid, vol. 3, no. 4, 2012, pp. 1977–1987. doi:10.1109/tsg.2012.2205952

[19] X. Yu, A. M. Khambadkone, H. Wang, S. T. S. Terence, "Control of parallel-connected power converters for low-voltage microgrid - Part I: A hybrid control architecture," IEEE Transactions on Power Electronics, vol. 25, no. 12, 2010, pp. 2962–2970. doi:10.1109/tpel.2010.2087393

[20] C. Chien-Liang, Y. Wang, J. -S. Lai, "Design of parallel inverters for smooth mode transfer microgrid applications," IEEE Transactions on Power Electronics, vol. 25, no. 1, 2010, pp. 6–15. doi:10.1109/tpel.2009.2025864

[21] J. He, Y. W. Li, D. Bosnjak, B. Harris, "Investigation and active damping of multiple resonances in a parallel-inverter-based microgrid," IEEE Transactions on Power Electronics, vol. 28, no. 1, 2013, pp. 234–246. doi:10.1109/tpel.2012.2195032

[22] U. B. Tayab, M. A. Bin Roslan, L. J. Hwai, M. Kashif, "A review of droop control techniques for microgrid," Renewable and Sustainable Energy Reviews, vol. 76, 2017, pp. 717–727. doi:10.1016/j.rser.2017.03.028

[23] S. D. Veeraganti, R. Nittala, "Operation of microgrid and control strategies," Research Anthology on Smart Grid and Microgrid Development, 2022, pp. 111–126. doi:10.4018/978-1-6684-3666-0.ch006

[24] N. Jayawarna, X. Wu, Y. Zhang, N. Jenkins, M. Barnes, "Stability of a microgrid," 3rd IET International Conference on Power Electronics, Machines and Drives (PEMD 2006), 2006. doi:10.1049/cp:20060123

[25] R. Heydari, Y. Khayat, M. Naderi, A. Anvari-Moghaddam, T. Dragicevic, F. Blaabjerg, "A decentralized adaptive control method for frequency regulation and power sharing in autonomous microgrids," 2019 IEEE 28th International Symposium on Industrial Electronics (ISIE), 2019. doi:10.1109/isie.2019.8781102

[26] C. N. Rowe, T. J. Summers, R. E. Betz, T. G. Moore, C. D. Townsend, "Implementing the virtual output impedance concept in a three phase system utilising cascaded Pi controllers in the DQ rotating reference frame for microgrid inverter control," 15th European Conference on Power Electronics and Applications (EPE), 2013. doi:10.1109/epe.2013.6634691

[27] T. V. Vu, D. Perkins, F. Diaz, D. Gonsoulin, C. S. Edrington, T. El-Mezyani, "Robust adaptive droop control for dc microgrids," Electric Power Systems Research, vol. 146, 2017, pp. 95–106. doi:10.1016/j.epsr.2017.01.021

[28] H. Shi, F. Zhuo, H. Yi, Z. Geng, "Control strategy for microgrid under three-phase unbalance condition," Journal of Modern Power Systems and Clean Energy, vol. 4, no. 1, 2016, pp. 94–102. doi:10.1007/s40565-015-0182-3

[29] L. Chia-Tse, C. -C. Chuang, C. -C. Chu, P. -T. Cheng, "Control strategies for distributed energy resources interface converters in the low voltage microgrid," 2009 IEEE Energy Conversion Congress and Exposition, 2009. doi:10.1109/ecce.2009.5316407

[30] L. Xiaodong, "Emerging power quality challenges due to integration of renewable energy sources," 2016 IEEE Industry Applications Society Annual Meeting, 2016. doi:10.1109/ias.2016.7731973

[31] S. Gheorghe, N. Golovanov, G. C. Lazaroiu, C. Stanescu, G. Gheorghe, "The connection of renewable sources to the grid. Influences and power quality issues," 10th International Symposium on Advanced Topics in Electrical Engineering (ATEE), 2017. doi:10.1109/atee.2017.7905148

[32] J. C. Vasquez, J. M. Guerrero, M. Savaghebi, J. Eloy-Garcia, R. Teodorescu, "Modeling, analysis, and design of stationary-reference-frame droop-controlled parallel three-phase voltage source inverters," IEEE Transactions on Industrial Electronics, vol. 60, no. 4, 2013, pp. 1271–1280. doi:10.1109/tie.2012.2194951

[33] X. Pan, W. Li, X. Chen, K. Qu, J. Zhao, T. Ye, "Analysis and evaluation of the decoupling control strategies for the design of grid-connected inverter with LCL filter," International Conference on Renewable Power Generation (RPG 2015), 2015, pp. 1-6. doi:10.1049/cp.2015.0530

[34] J. M. Guerrero, J. C. Vásquez, R. Teodorescu, "Hierarchical control of droop-controlled AC and DC microgrids—A general approach toward standardization," IEEE Transactions on Industrial Electronics, vol. 58, no. 1, 2011, pp. 158–172. doi:10.1109/tie.2010.2066534

[35] W. Yao, M. Chen, J. Matas, J. M. Guerrero, Z. -M. Qian, "Design and analysis of the droop control method for parallel inverters considering the impact of the complex impedance on the power sharing," IEEE Transactions on Industrial Electronics, vol. 58, no. 2, 2011, pp. 576–588. doi:10.1109/tie.2010.2046001

[36] R. A. Mastromauro, M. Liserre, A. Dell'Aquila, J. M. Guerrero, J. C. Vasquez, "Droop control of a multifunctional PV inverter," In 2008 IEEE International Symposium on Industrial Electronics, pp. 2396-2400. IEEE, 2008. doi:10.1109/ISIE.2008.4677145